

Testing Radiative Neutrino Mass Generation at the LHC

Chian-Shu Chen, Chao-Qiang Geng

Department of Physics, National Tsing Hua University, Hsinchu, Taiwan 300

John N. Ng, Jackson M. S. Wu

Theory Group, TRIUMF, 4004 Wesbrook Mall, Vancouver, B.C. Canada V6T 2A3

ABSTRACT: We investigate in detail a model that contains an additional $SU(2)$ singlet and triplet scalar fields than the Standard Model (SM). This allows the radiative generation of Majorana neutrino masses at two-loop order with the help of doubly charged Higgs bosons that arise from the extended Higgs sector. The phenomenology of the Higgs and neutrino sectors of the model is studied. We give the analytical form of the masses of scalar and pseudoscalar bosons and their mixings, and the structure of the active neutrino mass matrix. It is found that the model accommodates only normal neutrino mass hierarchy, and that there is a large parameter space where the doubly charged Higgs can be observed at the Large Hadron Collider (LHC), thereby making it testable at the LHC. Furthermore, the neutrino-less double beta ($0\nu\beta\beta$) decays arise predominantly from exchange processes involving the doubly charged Higgs, whose existence is thus unmistakable if $0\nu\beta\beta$ decays are observed. The production and decays of the doubly charged Higgs are analyzed, and distinct and distinguishing signals are discussed.

KEYWORDS: Neutrino Mass, Doubly Charged Higgs, LHC.

Contents

1. Introduction	1
2. A minimal model with radiative neutrino mass generation.	2
3. Neutrino phenomenology and constraints	7
3.1 Two-loop neutrino masses and neutrino oscillations	7
3.2 Rare muon and τ decays	11
3.3 $0\nu\beta\beta$ decays of nuclei	13
4. Doubly Charged Higgs at the LHC	14
4.1 Production of the doubly charged Higgs	14
4.2 The decay of $P_1^{\pm\pm}$	16
5. Conclusion	19

1. Introduction

The origin of small active neutrino masses remains one of the most challenging problem in physics. The small neutrino masses generated through the seesaw mechanism is popularly viewed as heralding new physics at scales larger than 10^{12} GeV, and thus provide a window to Grand Unified Theories (GUTs) with or without supersymmetry. Crucial to the construction is the introduction of heavy Standard Model (SM) singlet fermions commonly known as sterile neutrinos.

Recently, the idea of extra spatial dimensions together with brane world scenarios offers a very different perspective to the question of neutrino masses. Here their smallness results from either the suppression factors associated with the relatively large extra dimensions, or from the small overlap between the wave functions of the sterile neutrinos in the extra dimensions.

It is interesting to note that these different perspectives can be incorporated into a single framework in brane world scenarios; a recent discussion can be found in [1]. However the existence of sterile neutrinos is required in both constructions which, along with the value of their masses, are all important questions by themselves. To date the best information on light sterile neutrinos comes from cosmological considerations; direct experimental tests are very challenging due to the fact that they have no SM interactions.

It is well known that the masses of active neutrinos can be generated without sterile right-handed (RH) neutrinos via quantum loop effects. Without the RH states there are no Dirac couplings of the SM lepton doublet to the Higgs fields, and consequently the

active neutrinos can only have Majorana masses. The prototype model was constructed in [2] where there is an extended Higgs sector, and the gauge symmetry is that of the SM. Crucial to the construction was the use of an $SU(2)$ singlet Higgs field with a nontrivial hypercharge. Unfortunately the model gives rise to bimaximal neutrino mixings which is disfavored by the most recent neutrino data (for a recent review see [3]). More realistic neutrino masses can be obtained using doubly charged Higgs fields [4].

In our construction, we keep the SM gauge group and extend the Higgs sector by adding both an $SU(2)$ triplet and a doubly charged singlet field. We also postulate that lepton number violating effects take place only in the scalar potential, while the rest of the Lagrangian respect lepton number. A brief discussion of our model has already appeared in [5] where we showed how naturally small neutrino masses can arise from just two-loop radiative corrections. In this paper we will give a detail discussion of rich scalar phenomenology of the model. In particular the signals at the Large Hadron Collider (LHC) are investigated.

The rest of the paper is organized as follow. In Sec. 2 we describe in detail our model. We work out the constraints on the vacuum expectation value and other parameters that control the mass of the two physical doubly charged Higgs bosons $P_{1,2}^{\pm\pm}$. We show that at least one of the doubly charged Higgs can have mass at the electroweak scale if we demand the theory be perturbative up to the TeV scale. In Sec. 3 we discuss in detail the phenomenology of the neutrino sector in our model. We examine closely the neutrino mass matrix and the constraints from the oscillation data. We show that normal hierarchy arises naturally in our model, and we place constraints on the neutrino-lepton Yukawa couplings. Lastly, we discuss the implications these constraints have on the $0\nu\beta\beta$ decays of nuclei in our model. In Sec. 4 we discuss the phenomenology of the doubly charged Higgs production at the LHC, and their decays. We show that the decay pattern of the doubly charged Higgs in our model can be very different, and can therefore be used to distinguish our model from others that also contain doubly charged Higgs. Sec. 5 contains our conclusions.

2. A minimal model with radiative neutrino mass generation.

The model is based on the SM gauge symmetry with an extended Higgs sector and minimal matter content. Group theory dictates that only $SU(2)$ singlets and triplets are allowed for the generation of Majorana masses for the neutrinos. Besides the SM Higgs doublet given by

$$\phi = \begin{pmatrix} \phi^0 \\ \phi^- \end{pmatrix}_{-1}, \quad \tilde{\phi} = i\tau_2\phi, \quad (2.1)$$

we introduce a complex triplet Higgs T represented by a 2×2 matrix

$$T = \begin{pmatrix} T^0 & \frac{T^-}{\sqrt{2}} \\ \frac{T^-}{\sqrt{2}} & T^{--} \end{pmatrix}_{-2}, \quad (2.2)$$

as well as a complex singlet scalar Ψ_4^{++} . The subscripts denote the weak hypercharges of the fields as given by the relation $Q = T_3 + \frac{1}{2}Y$. The most general potential for the scalar

fields is given by

$$\begin{aligned}
V(\phi, T, \psi) = & -\mu^2 \phi^\dagger \phi + \lambda_\phi (\phi^\dagger \phi)^2 - \mu_T^2 \text{Tr}(T^\dagger T) + \lambda_T [\text{Tr}(T^\dagger T)]^2 + \lambda'_T \text{Tr}(T^\dagger T T^\dagger T) \\
& + m^2 \Psi^\dagger \Psi + \lambda_\Psi (\Psi^\dagger \Psi)^2 + \kappa_1 \text{Tr}(\phi^\dagger \phi T^\dagger T) + \kappa_2 \phi^\dagger T T^\dagger \phi + \kappa_\Psi \phi^\dagger \phi \Psi^\dagger \Psi \\
& + \rho \text{Tr}(T^\dagger T \Psi^\dagger \Psi) + \left[\lambda (\tilde{\phi}^T T \tilde{\phi} \Psi) - M(\phi^T T^\dagger \phi) + h.c. \right]. \tag{2.3}
\end{aligned}$$

One can assign Ψ a lepton number 2, and T a lepton number 0. Then terms in the square brackets at the end of Eq. (2.3) contain lepton number violating interactions. We will take both μ^2 , μ_T^2 to be positive so that spontaneous symmetry breaking (SSB) takes place. Minimizing the potential gives us the VEVs: $\langle \phi^0 \rangle \equiv \frac{v}{\sqrt{2}}$ and $\langle T^0 \rangle \equiv \frac{v_T}{\sqrt{2}}$.

With the additional fields T and Ψ , two new Yukawa terms can be constructed that are allowed by the gauge symmetry. The first is $Y_{ab} \bar{l}_{aR}^c l_{bR} \Psi$, which is lepton number conserving. Here a, b are family indices and l_a is a lepton singlet. The second is LLT that violates lepton number, which we assume not to occur at the tree level*. The absence of this term frees one from having to put in by hand a very small value of v_T in the eV range that plagues other Higgs models of neutrino masses. Adding in the SM terms and the covariant derivatives of T and Ψ we have a complete renormalizable model.

From Eq. (2.3) it can be seen that the various Higgs fields will mix among themselves. In particular, the pair $\Re \phi^0$ and $\Re T^0$ will mix that give rise to two physical neutral scalars, h^0 and P^0 , and the pair $\Im \phi^0$ and $\Im T^0$ will mix with one combination that is eaten by the Z boson to leave a physical pseudoscalar T_a^0 . Similarly for the charged states ϕ^\pm and T^\pm , one combination will be eaten by the W bosons leaving only a pair of singly charged P^\pm scalars. Finally the weak eigenstates $T^{\pm\pm}$ and $\Psi^{\pm\pm}$ will also mix to form physical states $P_1^{\pm\pm}$ and $P_2^{\pm\pm}$, with the mixing angle denoted by δ , and masses M_1 and M_2 respectively. All the masses and mixing angles are free parameters in our model, which we can use to replace some of the parameters in $V(\phi, T, \Psi)$. They are to be determined experimentally. In summary, the physical spin 0 particles consist of a pair of singly charged bosons, P^\pm , two pairs of doubly charged bosons $P_1^{\pm\pm}$ and $P_2^{\pm\pm}$, a pair of Higgs scalars h^0 and P^0 , and a pseudoscalar A^0 .

The value of v_T is constrained by the electroweak phenomenology. After the electroweak symmetry breaking, the W and Z bosons pick up masses at the tree level given by

$$M_W^2 = \frac{g^2}{4}(v^2 + 2v_T^2), \quad M_Z^2 = \frac{g^2}{4 \cos^2 \theta_W}(v^2 + 4v_T^2), \tag{2.4}$$

where we have used standard notations, and the tree level relation $e = g \sin \theta_W$ holds. From the Particle Data Group (PDG) we have $\rho = 1.002_{-0.0009}^{+0.0007}$ [6] and $M_W = 80.41$ GeV [7]. This implies that $v_T < 4.41$ GeV. We will see below that this is a controlling scale for the neutrino masses.

*There are several ways to naturally suppress the Yukawa couplings of $L_a L_b T$. One way is to embed the model in a 5-dimensional set-up and compactify the extra dimensions on an orbifold S_1/Z_2 . The lepton and Higgs fields are then assigned with different orbifold parities to forbid the LLT term while still allows the $ll\psi$ term. Another way is to further extend the Higgs sector by including a second Higgs doublet and then employ an appropriate discrete symmetry. The LLT term will be generated radiatively after symmetry breaking, but is small.

In the limit where $\lambda, M \rightarrow 0$ the model conserves lepton number, and is thus technically natural. Since λ is a dimensionless coupling, it is expected to be of order unity ($< 4\pi$) so that perturbation is valid, which is assumed throughout this paper. The value of M is important in setting the scale of lepton number violation. It enters in the conditions for minimizing the scalar potential $V(\phi, T, \Psi)$:

$$-\mu^2 + \lambda_\phi v^2 + \frac{1}{2}\kappa_+ v_T^2 - \sqrt{2}Mv_T = 0, \quad (2.5)$$

$$-\mu_T^2 + \lambda_+ v_T^2 + \frac{1}{2}\kappa_+ v^2 - \frac{v^2}{\sqrt{2}} \left(\frac{M}{v_T} \right) = 0, \quad (2.6)$$

where $\kappa_+ = \kappa_1 + \kappa_2$ and $\lambda_+ = \lambda_T + \lambda'_T$. Taking v to be of the electroweak scale and $v_T/v \approx 0.02$, the interesting limiting cases are:

- A. $M \sim v_T$: The minimum conditions, Eq. (2.5), can be naturally satisfied without fine tuning between the parameters if $\mu_T \sim v_T$.
- B. $M \sim v \gg v_T$: To satisfy the minimum conditions, $\mu_T^2 \sim v^3/v_T$ is required. This appears to be unnatural although not forbidden.
- C. $M > v$: The minimum conditions can only be satisfied by tuning the dimensionful and/or the dimensionless couplings. We will not consider this case.

For convenience define $\omega \equiv \frac{M}{\sqrt{2}v_T}$. Then Case A and B correspond to $\omega \sim 1$ and $\omega \gg 1$ respectively. Qualitatively, we see that $\omega \lesssim 1$ is more natural in our model. We will therefore concentrate mostly in this region of the parameter space below.

We now turn to the masses of the physical scalar and pseudoscalar particles in our model. The mass of the singly charged Higgs boson is given by

$$M_{P^\pm}^2 = \left(\omega - \frac{\kappa_2}{4} \right) (v^2 + 2v_T^2). \quad (2.7)$$

For $\omega \sim 1$, we expect the charged Higgs to have mass in the 100 to 1000 GeV range.

For the two doubly charged scalars, their masses are given by

$$M_{P_{1,2}}^2 = \frac{1}{2} \left[a + c \mp \sqrt{4b^2 + (c-a)^2} \right], \quad (2.8)$$

where the P_1 state takes the upper sign, and

$$a = \frac{1}{2}(2\omega - \kappa_2)v^2 - \lambda'_T v_T^2, \quad b = \frac{1}{2}\lambda v^2, \quad c = m^2 + \frac{1}{2}(\kappa_\Psi v^2 + \rho v_T^2). \quad (2.9)$$

Note that m ($m^2 > 0$) is a mass parameter for the singlet and should not be confused with the physical mass. As such it is in general not constrained.

Consider now Case A. In the limit where m is large ($m \gg v$), we have from Eqs. (2.8) and (2.9):

$$M_{P_1}^2 = \frac{1}{2}(2\omega - \kappa_2)v^2 - \lambda'_T v_T^2 + \mathcal{O}\left(\frac{v^4}{m^2}\right), \quad (2.10)$$

$$M_{P_2}^2 = m^2 + \frac{1}{2}(\kappa_\Psi v^2 + \rho v_T^2) + \mathcal{O}\left(\frac{v^4}{m^2}\right). \quad (2.11)$$

We see in this limit, M_{P_1} saturates to an m -independent value, $\sqrt{\frac{1}{2}(2\omega - \kappa_2)v^2 - \lambda'_T v_T^2}$, which is also its maximal value for a given set of model parameters. On the other hand, M_{P_2} increases as m , which means the P_2 state will be too heavy to be of interest to the LHC in the large m limit.

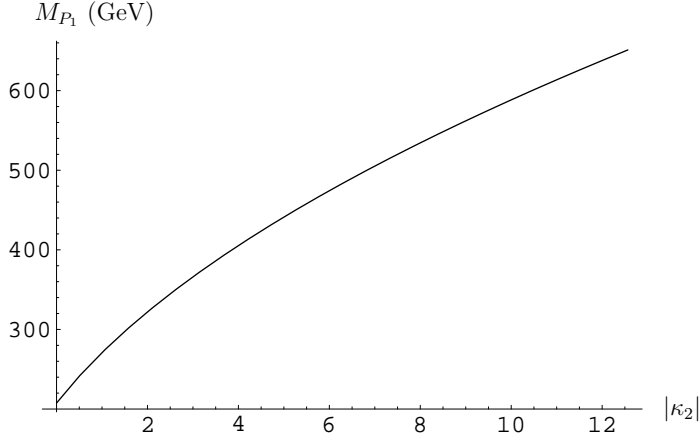


Figure 1: Maximum value of M_{P_1} for $v_T = M = 4$ GeV, and $|\lambda'_T|$ set to 4π .

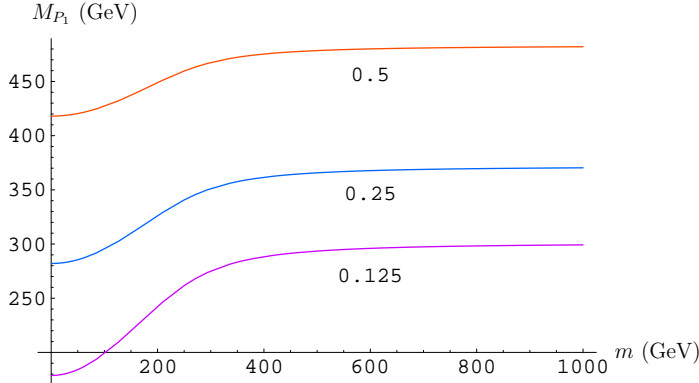


Figure 2: M_{P_1} as a function of m for $|\kappa_2| = 0.5, 0.25, 0.125$ in units of 4π , with $v_T = M = 4$ GeV and $\lambda = -\lambda'_T = 1$.

In Fig. 1 we plot the maximal value of M_{P_1} as a function of $|\kappa_2| = -\kappa_2$, with v_T and M set to 4 GeV. The coupling λ'_T is set to $|\lambda'_T| = -\lambda'_T = 4\pi$, the upper limit under which perturbation is expected to be valid. In Fig. 2 we plot M_{P_1} as a function of m for three different values of $|\kappa_2|$, with all dimensionless couplings kept perturbative. We see clearly here the saturation of M_{P_2} at large values of m . Figs. 1 and 2 show that the mass range of the P_1 state is well within the reach of the LHC, its existence is thus a testable feature of our model at the LHC.

Note that if we take the opposite limit where $m \rightarrow 0$, two weak scale doubly charged scalars are possible. For example, if we take $\omega = 1$, $\lambda = 1$, $\kappa_\Psi = -\kappa_2 = 2$, and $\rho = 2\lambda'_T = 2$, we get $M_{P_1} = 219.3$ GeV and $M_{P_2} = 365.8$ GeV. However, this will not hold in Case B. In

this case the P_2 state will be heavy with mass above a TeV, while the P_1 state remains at the weak scale.

The doubly charged scalars form a two-level system in which the mass and weak eigenstates are related by

$$\begin{pmatrix} P_1^{\pm\pm} \\ P_2^{\pm\pm} \end{pmatrix} = \begin{pmatrix} \cos \delta & \sin \delta \\ -\sin \delta & \cos \delta \end{pmatrix} \begin{pmatrix} T^{\pm\pm} \\ \Psi^{\pm\pm} \end{pmatrix}. \quad (2.12)$$

The mixing angle δ is a measurable physical parameter. It is given by

$$\begin{aligned} \sin 2\delta &= \left[1 + \frac{(c-a)^2}{4b^2} \right]^{-\frac{1}{2}} \\ &= \left[1 + \left(\frac{2m^2 + (2\lambda'_T + \rho)v_T^2}{2\lambda v^2} + \frac{\kappa_2 + \kappa_\Psi}{2\lambda} - \frac{\omega}{\lambda} \right)^2 \right]^{-\frac{1}{2}}, \end{aligned} \quad (2.13)$$

where a , b and c are those given in Eq. (2.9). For Case A, if $m^2 \lesssim v^2$, the mixing can be large and close to maximal. But if $m^2 \gg v^2$, the mixing will be small, which is expected since the two states are widely split. For case B, large mixing can be achieved only if a cancellation occurs between the various parameter in Eq. (2.13).

We now turn to the three physical neutral scalar bosons in our model. The pseudoscalar T_a^0 has mass given by

$$M_{T_a^0}^2 = \frac{1}{2}\omega(v^2 + 4v_T^2). \quad (2.14)$$

Note that if $\omega \rightarrow 0$, T_a^0 becomes a Majoron.

The masses of the neutral scalars h^0 and P^0 again have the general form

$$M_{h^0, P^0}^2 = \frac{1}{2} \left[a' + c' \mp \sqrt{4b'^2 + (c' - a')^2} \right], \quad (2.15)$$

where the h^0 state takes the upper sign, and

$$a' = \lambda_\phi v^2, \quad b' = \left(\frac{1}{2}\kappa_+ - \omega \right) v v_T, \quad c' = \lambda_+ v_T^2 + \frac{1}{2}\omega v^2. \quad (2.16)$$

The physical neutral scalars also form a two-level system in which the mass and weak eigenstates mix, with the mixing angle, ϑ given by

$$\begin{aligned} \sin 2\vartheta &= \left[1 + \frac{(c' - a')^2}{4b'^2} \right]^{-\frac{1}{2}} \\ &= \left[1 + \frac{v^2}{16v_T^2} \left(\frac{2\lambda_+}{\kappa_+ - 2\omega} \frac{v_T^2}{v^2} + \frac{\omega - 2\lambda_\phi}{\kappa_+ - 2\omega} \right)^2 \right]^{-\frac{1}{2}}. \end{aligned} \quad (2.17)$$

It can be seen that ϑ is of order v_T/v for both Case A and B.

For Case A, T_a^0 and P^0 can both be light and almost degenerate. If they are lighter than half the Z boson mass they will contribute to its invisible width [8]:

$$\Gamma(Z^0 \rightarrow P^0 T_a^0) = \frac{G_F M_Z^3}{6\sqrt{2}\pi} \left(1 - 2 \frac{M_{P^0}^2 + M_a^2}{M_Z^2} \right)^3, \quad (2.18)$$

where the notation is standard. Demanding that this contributes less than 150 MeV to the invisible width we obtain $|\omega| > 0.016$. For Case B, all the neutral bosons have weak scale masses and the above limit does not apply. However, we still expect P^0 and T_a^0 to be close in mass.

We summarize our findings on the masses of the scalar and pseudoscalar bosons in our model:

- A. $M \sim v_T$: The mass of $P_{1,2}^{\pm\pm}$ is expected to be greater than 200 GeV if $m \lesssim 1$ TeV. But if m is much larger than that, the mass of $P_1^{\pm\pm}$ will saturate to a constant value which is at most $\mathcal{O}(600)$ GeV; the $P_2^{\pm\pm}$ states are expected to be very heavy in the large m limit. The singly charged Higgs has a mass at the weak scale that is m -independent. The masses of neutral Higgs-like bosons are also of the weak scale. Being the would-be Majoron, T_a^0 provides a bound on ω : $|\omega| > 0.016$.
- B. $M \sim v \gg v_T$: Here, only the mass of $P_1^{\pm\pm}$ is expected to be at the weak scale. All the other scalars with the exception of h^0 (which is mostly a SM Higgs boson) will be too heavy to be of interest at the LHC, since their masses are controlled by ω .

3. Neutrino phenomenology and constraints

3.1 Two-loop neutrino masses and neutrino oscillations

A feature of our model is that neutrino masses are generated at the two-loop level, and the crucial couplings are the Yukawa terms. It is well known that the Yukawa couplings of ϕ to fermions are diagonalized by a biunitary transformation effected via U_L and U_R such that the charged leptons are mass eigenstates. Clearly, applying this transformation does not in general diagonalize Y_{ab} . Hence we expect flavor violating couplings Y'_{ab} between families of RH leptons and the physical P^{++} states.[†] Thus in general, the decay modes such as $P^{++} \rightarrow \mu^+ e^+$ must occur. The coupling of P^\pm to fermions, on the other hand, is similar to SM but scaled by a factor v_T/v .

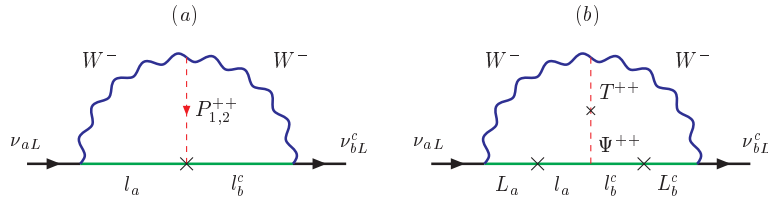


Figure 3: The two-loop diagram for the neutrino mass in: (a) the mass eigenbasis and (b) the weak eigenbasis.

The active neutrino mass matrix can now be calculated. The leading contribution is given by the two-loop Feynman diagram depicted in Fig. 3. After a standard but lengthy

[†]In the following we assume that the charged leptons are in the mass basis, and so $Y' = U_R Y U_R$. For notational simplicity we will drop the prime henceforth.

calculation we find

$$(m_\nu)_{ab} = \frac{1}{\sqrt{2}} g^4 m_a m_b v_T Y_{ab} \sin(2\delta) [I(M_W^2, M_{P_1}^2, m_a, m_b) - I(M_W^2, M_{P_2}^2, m_a, m_b)] , \quad (3.1)$$

where $a, b = e, \mu, \tau$. The integral I is given by

$$I(M_W^2, M_{P_i}^2, m_a^2, m_b^2) = \int \frac{d^4 q}{(2\pi)^4} \int \frac{d^4 k}{(2\pi)^4} \frac{1}{k^2 - m_a^2} \frac{1}{k^2 - M_W^2} \frac{1}{q^2 - M_W^2} \frac{1}{q^2 - m_b^2} \frac{1}{(k-q)^2 - M_{P_i}^2} . \quad (3.2)$$

The integral can be evaluated analytically as in [9]. Note that there is a generalized GIM mechanism at work here. This can be seen clearly in the limit $M_{P_{1,2}} > M_W$ [10]:

$$I(M_W^2, M_{P_i}^2, 0, 0) \sim \frac{1}{(4\pi)^4} \frac{1}{M_{P_i}^2} \log^2 \left(\frac{M_W^2}{M_{P_i}^2} \right) . \quad (3.3)$$

We see that not only is the neutrino mass two-loop suppressed, there is also a helicity suppression from the charged lepton masses, whose origin can be clearly seen from Fig. 3(b). It is clear that the internal lepton lines must have mass insertions since Ψ^{++} only couples to RH leptons. As a result, $(m_\nu)_{ee}$ will be vanishingly small. This has important consequences in $0\nu\beta\beta$ decays as well as the choice of signatures for the detection of these scalars at the LHC.

Explicitly, the neutrino mass matrix is given by

$$\begin{aligned} m_\nu &= \tilde{f}(M_{P_1}, M_{P_2}) \times \begin{pmatrix} m_e^2 Y_{ee} & m_e m_\mu Y_{e\mu} & m_e m_\tau Y_{e\tau} \\ m_e m_\mu Y_{e\mu} & m_\mu^2 Y_{\mu\mu} & m_\tau m_\mu Y_{\mu\tau} \\ m_e m_\tau Y_{e\tau} & m_\tau m_\mu Y_{\mu\tau} & m_\tau^2 Y_{\tau\tau} \end{pmatrix} \\ &= f(M_{P_1}, M_{P_2}) \times \begin{pmatrix} 2.6 \times 10^{-7} Y_{ee} & 5.4 \times 10^{-5} Y_{e\mu} & 9.1 \times 10^{-4} Y_{e\tau} \\ 5.4 \times 10^{-5} Y_{e\mu} & 1.1 \times 10^{-2} Y_{\mu\mu} & 0.19 Y_{\mu\tau} \\ 9.1 \times 10^{-4} Y_{e\tau} & 0.19 Y_{\mu\tau} & 3.17 Y_{\tau\tau} \end{pmatrix} , \end{aligned} \quad (3.4)$$

where

$$\tilde{f}(M_{P_1}, M_{P_2}) = \frac{\sqrt{2} g^4 v_T \sin(2\delta)}{128\pi^4} \left[\frac{1}{M_{P_1}^2} \log^2 \left(\frac{M_W}{M_{P_1}} \right) - \frac{1}{M_{P_2}^2} \log^2 \left(\frac{M_W}{M_{P_2}} \right) \right] , \quad (3.5)$$

and $f = \tilde{f} \times (1\text{GeV}^2)$ gives a qualitatively estimate of the overall scale of active neutrino masses. Now for normal hierarchy, the neutrino mass matrix has the following structure

$$\begin{pmatrix} \varepsilon' & \varepsilon & \varepsilon \\ \varepsilon & 1 + \eta & 1 + \eta \\ \varepsilon & 1 + \eta & 1 + \eta \end{pmatrix} , \quad (3.6)$$

where $\varepsilon, \varepsilon'$ and $\eta \ll 1$. Comparing Eq. (3.4) to Eq. (3.6), we see there is a qualitatively agreement.

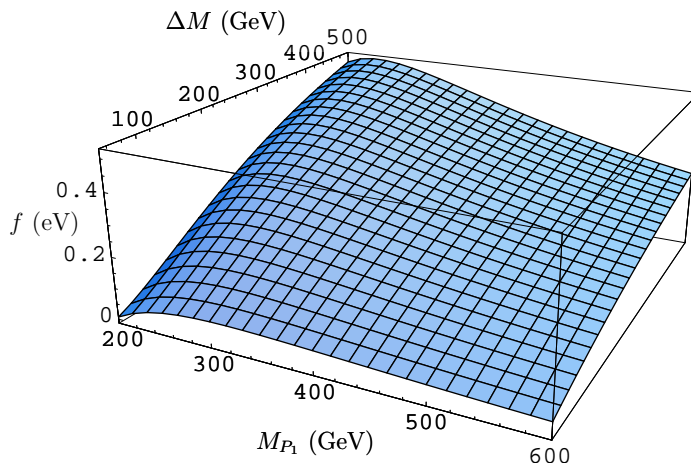


Figure 4: The scale $f(M_{P_1}, M_{P_2})$ as a function of M_{P_1} and the mass difference $\Delta M = M_{P_2} - M_{P_1}$ for $\sin 2\delta = 0.5$ and $v_T = 4$ GeV.

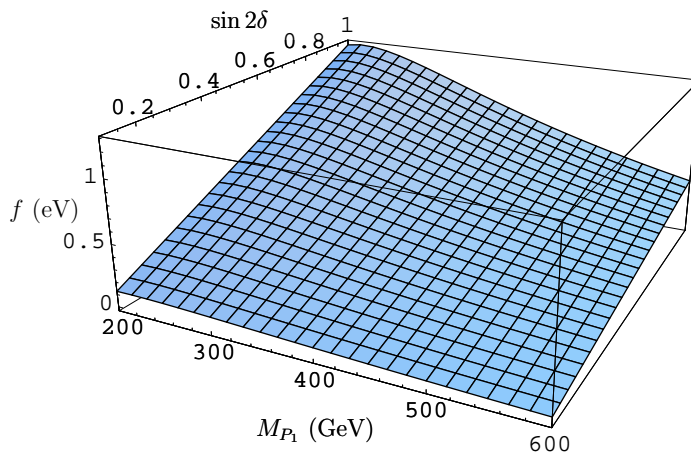


Figure 5: The scale $f(M_{P_1}, M_{P_2})$ as a function of M_{P_1} and $\sin 2\delta$ for $M_{P_2} = 1$ TeV and $v_T = 4$ GeV.

We plot the behavior of $f(M_{P_1}, M_{P_2})$ as a function of M_{P_1} and $\Delta M = M_{P_2} - M_{P_1}$ in Fig. 4. The range of parameters used is applicable to Case A. We see that overall, the neutrino mass increases as the mass difference of the two doubly charged scalar increases. In Fig. 5 we plot the behavior of $f(M_{P_1}, M_{P_2})$ for parameter range applicable to Case B. In both cases we expect neutrino masses to be in the sub-eV range.

We proceed next to examine how the neutrino oscillation data can constrain our model. Neutrino oscillations depend on the difference of mass-squared, hence we will focus on m_ν^2 accordingly. Since the eigenvalues of m_ν^2 are in general complex, and it is customary to separate out a phase matrix, we write

$$m_\nu^2 = V_{PMNS}^T U \begin{pmatrix} m_1^2 & 0 & 0 \\ 0 & m_2^2 & 0 \\ 0 & 0 & m_3^2 \end{pmatrix} U V_{PMNS}, \quad U = \begin{pmatrix} 1 & 0 & 0 \\ 0 & e^{i\varphi_1} & 0 \\ 0 & 0 & e^{i(\varphi_2+\alpha)} \end{pmatrix}, \quad (3.7)$$

where V_{PMNS} is the neutrino mixing matrix [11] and in standard notation is the same as

the quark mixing matrix [6], whereas α is the Dirac phase. For normal hierarchy, we have $m_1 \simeq 0$, $m_2^2 \simeq \Delta m_{\odot}^2$, and $m_3^2 \simeq \Delta m_{atm}^2$. Oscillation experiments currently place limits on the following relevant parameters [3]:

$$\begin{aligned} 7.1 \times 10^{-5} < \Delta m_{\odot}^2 < 8.9 \times 10^{-5} \text{ (eV}^2\text{)}, & \quad 0.164 < \sin^2 \theta_{12} < 0.494, \\ 1.4 \times 10^{-3} < |\Delta m_{atm}^2| < 3.3 \times 10^{-3} \text{ (eV}^2\text{)}, & \quad 0.22 < \sin^2 \theta_{23} < 0.85, \\ \sin^2 2\theta_{13} = 0 \pm 0.04. & \end{aligned} \quad (3.8)$$

Using Eqs. (3.4) and (3.7) and the oscillation data we can get six constraints on the elements of m_ν^2 . From the first row of m_ν^2 we obtain

$$f^2 Y_{e\tau}^2 \leq 1.32 \times 10^2 \text{ eV}^2, \quad f^2 Y_{e\tau} Y_{\mu\tau} \leq 1 \text{ eV}^2, \quad f^2 Y_{e\tau} Y_{\tau\tau} \leq 9.0 \times 10^{-2} \text{ eV}^2. \quad (3.9)$$

Since the phases involved are unknown, we do not get lower bounds for these quantities. As will be seen below, the bounds given in Eq. (3.9) are very loose compared to that found from rare muon and τ decays. The remaining three constraints are more stringent relatively, and they came by demanding a good fit to normal hierarchy:

$$f^2(Y_{\mu\mu}^2 + 300Y_{\mu\tau}^2) \leq 2.7 \text{ eV}^2, \quad (3.10)$$

$$f^2(Y_{\mu\mu} + 285Y_{\tau\tau})Y_{\mu\tau} \leq 2.4 \times 10^{-1} \text{ eV}^2, \quad (3.11)$$

$$f^2(Y_{\mu\tau}^2 + 278Y_{\tau\tau}^2) \leq 2.9 \times 10^{-2} \text{ eV}^2. \quad (3.12)$$

Using Eqs. (3.11) and (3.12), we plot in Fig. 6 the allowed parameter space for $Y_{\mu\tau}$ and $Y_{\tau\tau}$, with f set to 0.5 eV. [‡]

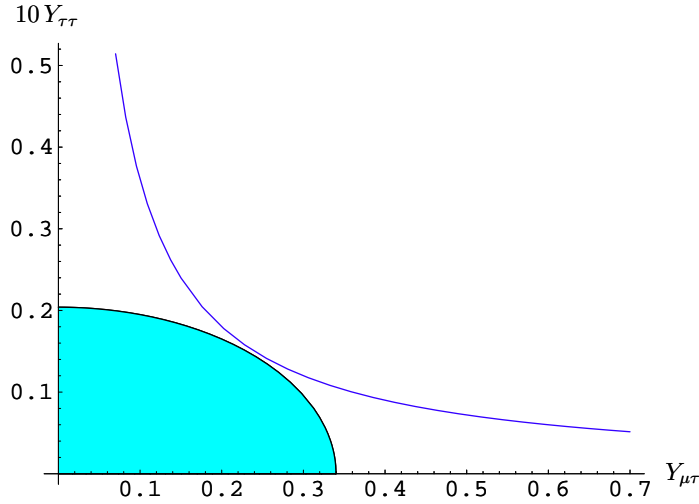


Figure 6: Parameter space allowed for $Y_{\tau\tau}$ and $Y_{\mu\tau}$ for $f = 0.5$ eV. The hyperbolic curve is the upper limit set by Eq. (3.11). The shaded region is that allowed by both Eq. (3.11) and Eq. (3.12).

[‡]In plotting Fig. 6, we have used the fact that $Y_{\mu\mu}Y_{\mu\tau} \ll 0.24$, which we show below.

3.2 Rare muon and τ decays

The doubly charged Higgs bosons lead to many lepton number violating processes. Since no such signals were found in current experiments, they lead to very strong constraints on the Yukawa couplings. In the following, we work out these constraints.

A. Muonium anti-muonium conversion

The effective Hamiltonian is given by the $P_{1,2}^{--}$ exchange at tree level:

$$H_{M\bar{M}} = \frac{Y_{ee}Y_{\mu\mu}}{2M_{--}^2} \bar{\mu}\gamma^\mu e_R \bar{\mu}\gamma_\mu e_R + h.c. , \quad (3.13)$$

where M_{--} is the reduced mass of the pair of doubly charged Higgs given by

$$\frac{1}{M_{--}^2} = \frac{\sin^2 \delta}{M_{P_1}^2} + \frac{\cos^2 \delta}{M_{P_2}^2} . \quad (3.14)$$

The current experimental limit [6] gives

$$Y_{ee}Y_{\mu\mu} < 2.0 \times 10^{-3} (M_{--}/100 \text{ GeV})^2 . \quad (3.15)$$

B. Effective $e^+e^- \rightarrow l^+l^-$, $l = e, \mu, \tau$, contact interactions

The effective Hamiltonian for Bhabha scattering is

$$\frac{Y_{ee}^2}{M_{--}^2} \bar{e}_R \gamma^\mu e_R \bar{e}_R \gamma_\mu e_R . \quad (3.16)$$

The bounds are

$$\begin{aligned} Y_{ee}^2 &< 1.8 \times 10^{-3} (M_{--}/100 \text{ GeV})^2 , \\ Y_{e\mu}^2 &< 2.4 \times 10^{-3} (M_{--}/100 \text{ GeV})^2 , \\ Y_{e\tau}^2 &< 2.4 \times 10^{-3} (M_{--}/100 \text{ GeV})^2 . \end{aligned} \quad (3.17)$$

C. Rare $\mu \rightarrow 3e$ decays and its τ counterparts

These decays can all be induced at the tree level and thus provide the most stringent limits on the Yukawa couplings. For $\mu \rightarrow 3e$, the branching ratio is given by

$$Br(\mu \rightarrow 3e) = \left(\frac{Y_{e\mu}Y_{ee}}{g^2} \right)^2 \left(\frac{M_W}{M_{--}} \right)^4 , \quad (3.18)$$

with similar equations for τ decays. The constraints imposed by the data is given by

$$\begin{aligned} Y_{e\mu}Y_{ee} &< 6.6 \times 10^{-7} (M_{--}/100 \text{ GeV})^2 , \\ Y_{e\tau}Y_{ee} &< 3.0 \times 10^{-4} (M_{--}/100 \text{ GeV})^2 , \\ Y_{e\tau}Y_{\mu\mu} &< 3.0 \times 10^{-4} (M_{--}/100 \text{ GeV})^2 , \\ Y_{\mu\tau}Y_{\mu\mu} &< 2.9 \times 10^{-4} (M_{--}/100 \text{ GeV})^2 , \\ Y_{\mu\tau}Y_{ee} &< 2.9 \times 10^{-4} (M_{--}/100 \text{ GeV})^2 . \end{aligned} \quad (3.19)$$

D. Radiative flavor violating charged leptonic decays

We consider here rare radiative decays of $\mu \rightarrow e\gamma$ and $\tau \rightarrow \mu(e)\gamma$. The fact that they are not seen to a very high precision make them of paramount importance for probing the physics of lepton flavor violation. The branching for $\mu \rightarrow e\gamma$ is calculated in [12] using an effective theory approach:

$$Br(\mu \rightarrow e\gamma) = \frac{\alpha}{3\pi G_F^2} \sum_{l=e,\mu,\tau} \left(\frac{Y_{l\mu} Y_{le}}{M_{--}^2} \right)^2 \quad (3.20)$$

with obvious substitutions for τ decays. The limits are given by

$$\begin{aligned} \sum_l Y_{l\mu} Y_{le} &< 1.5 \times 10^{-5} (M_{--}/100 \text{ GeV})^2, \\ \sum_l Y_{l\tau} Y_{le} &< 1.4 \times 10^{-3} (M_{--}/100 \text{ GeV})^2, \\ \sum_l Y_{l\tau} Y_{l\mu} &< 1.1 \times 10^{-3} (M_{--}/100 \text{ GeV})^2. \end{aligned} \quad (3.21)$$

Comparing the sets of constraints we find that Eq. (3.19) gives the strongest limits. Although the limits from contact interactions, Eq. (3.17), are less stringent, they are useful nonetheless as they constrain individual couplings. We illustrate in Fig. 7 how $Y_{e\tau}$ and Y_{ee} are restricted by both contact and rare decay experiments for a chosen value of the reduced mass $M_{--} = 400 \text{ GeV}$.

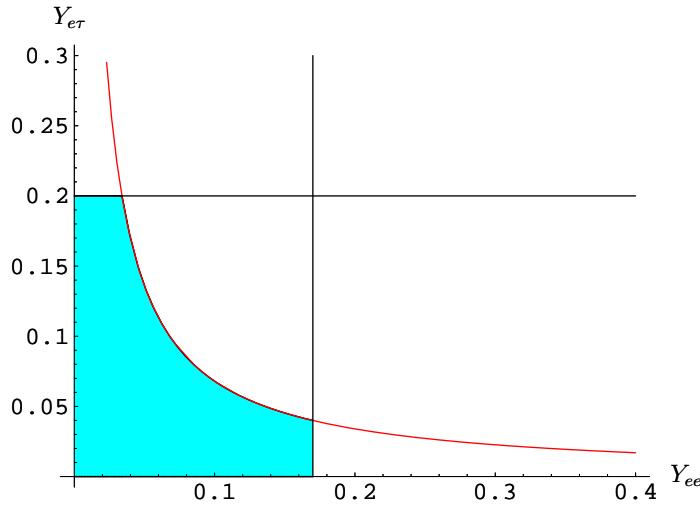


Figure 7: Parameter space allowed for $Y_{e\tau}$ and Y_{ee} (shaded). The straight lines are limits from the contact interactions, the hyperbolic curve the upper limit from $\tau \rightarrow 3e$ decays.

It is also interesting to compare the limits from the rare decays with that from neutrino oscillations. We plot in Fig. 8 the parameter space allowed in this case for $Y_{\mu\tau}$ and $Y_{\mu\mu}$, with $f = 0.5 \text{ eV}$ and $M_{--} = 400 \text{ GeV}$. Other comparisons are less instructive.

In summary, we have from contact interactions the upper limits

$$Y_{ee} < 0.17, \quad Y_{e\mu} < 0.2, \quad Y_{e\tau} < 0.2, \quad (3.22)$$

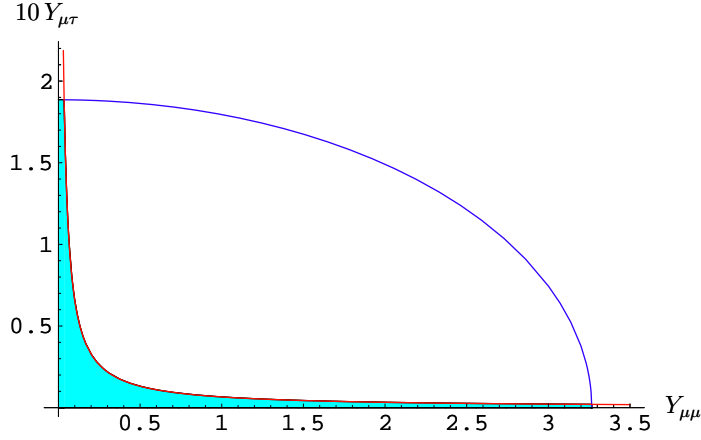


Figure 8: Parameter space allowed for for $Y_{\mu\tau}$ and $Y_{\mu\mu}$ (shaded). The hyperbolic curve is the upper limit from $\tau \rightarrow 3\mu$ decays, the ellipse the limit from fitting neutrino data.

and from neutrino data (see Fig. 6 and 8)

$$Y_{\mu\mu} < 3.5, \quad Y_{\mu\tau} < 0.2, \quad Y_{\tau\tau} < 0.02. \quad (3.23)$$

The values $M_{--} = 400$ GeV and $f = 0.5$ eV are used throughout in obtaining these limits. They are consistent with and typical of what can be expected for our model.

3.3 $0\nu\beta\beta$ decays of nuclei

In our model, $0\nu\beta\beta$ decays of nuclei are induced by the exchanges of virtual $P_{1,2}^{--}$ bosons and Majorana neutrino as depicted in Fig. 9. The quark level amplitude due to neutrino

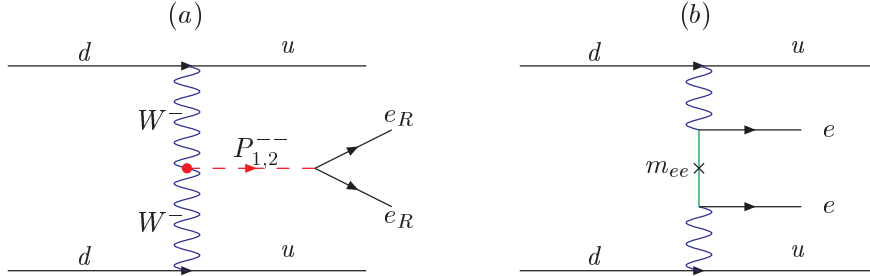


Figure 9: $0\nu\beta\beta$ decays via exchange of: (a) doubly charged Higgs and (b) light Majorana neutrinos.

exchanges is given by [§]

$$A_\nu \sim \frac{g^4}{M_W^4} \frac{m_{ee}}{\langle p \rangle^2}, \quad (3.24)$$

where $\langle p \rangle$ is the average momentum of the light neutrino exchanged. For notational simplicity we will drop the subscript ν for the mass matrix. Typically, $\langle p \rangle \sim 0.1$ GeV which reflects the long range nature of light particle exchanges. Note that there is a

[§]In our order of magnitude estimation, we have ignored spinor and kinematic factors, as well as factors from nuclear physics.

cancellation between the contributions from P_1 and P_2 , which is characteristic of a two level system.

The doubly charged Higgs exchange amplitude is given by

$$A_{P_{1,2}^{--}} \sim \frac{g^4 Y_{ee} v_T \sin 2\delta}{16\sqrt{2}M_W^4} \left(\frac{1}{M_{P_1}^2} - \frac{1}{M_{P_2}^2} \right), \quad (3.25)$$

where m_{ee} is given by Eq. (3.4). We estimate that $A_\nu/A_{P_{1,2}^{--}} \lesssim 10^{-7}$. The smallness of this ratio is due to the fact that in our model, m_{ee} is suppressed not only by a two-loop factor, it is also suppressed by the electron mass factor $(m_e/M_W)^2$ coming from the doubly charged scalar coupling. We conclude that if seen, $0\nu\beta\beta$ decays of nuclei will be due to the existence of doubly charged Higgs at the weak scale. This can be tested at the LHC, and is the subject of next section. Since there is no conclusive evidence for these decays, we use it to set a limit of Y_{ee} . The result is displayed in Fig. 10. It can be seen that the limit here is comparable to that from the contact interactions.

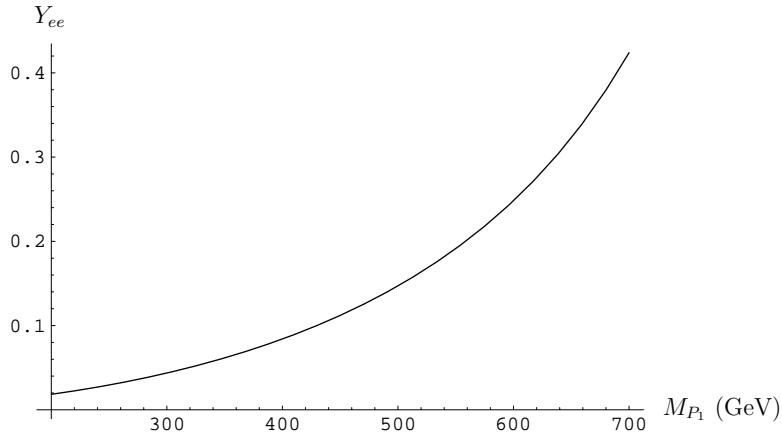


Figure 10: Upper limit on Y_{ee} as a function of M_{P_1} for $\sin 2\delta = 0.5$ and $M_{P_2} = 1$ TeV.

4. Doubly Charged Higgs at the LHC

4.1 Production of the doubly charged Higgs

A central ingredient in our neutrino mass generation is the two doubly charged Higgs, $P_{1,2}^{\pm\pm}$. We have argued that if not both, at least one of the doubly charged Higgs is well within reach of the LHC. Without loss of generality, we will take P_1 to be this (lighter) state, and focus on its production and decay below.

Now the doubly charged Higgs, $P_{1,2}^{\pm\pm}$, have no direct couplings to the quarks, which is characteristic of models with doubly charged scalars. However, they do couple to the SM gauge bosons. Thus at the LHC, $P_1^{\pm\pm}$ will be produced predominantly via the WW fusion processes, as illustrated in Fig. 9(a) (the d-quark is replaced by the u-quark for P_1^{++}), and the Drell-Yan (DY) annihilation processes,

$$q\bar{q} \rightarrow \gamma^*, Z^* \rightarrow P_1^{++} P_1^{--} \quad (q = u, d). \quad (4.1)$$

The relevant gauge-scalar couplings are given by ¶

$$\begin{aligned}
W_\mu^\pm W_\nu^\pm P_1^{\mp\mp} &: \frac{g^2}{\sqrt{2}} v_T c_\delta W_\mu^+ W_\nu^+ P_1^{--} + h.c. \\
A_\mu P_1^{++} P_1^{--} &: i 2e A_\mu \partial_\nu P_1^{++} P_1^{--} + h.c. \\
Z_\mu P_1^{++} P_1^{--} &: \frac{ig}{c_W} [(1 - 2s_W^2)c_\delta^2 - 2s_W^2 s_\delta^2] Z_\mu \partial_\nu P_1^{++} P_1^{--} + h.c.
\end{aligned} \tag{4.2}$$

where $g = e/\sin\theta_W$, $s_W \equiv \sin\theta_W$, $c_\delta \equiv \cos\delta$ and $s_\delta \equiv \sin\delta$.

We calculate the production cross sections numerically using the CalcHEP package [13], which allows an easy implementation of our model. The calculations are leading order, and are done in unitary gauge. The cross sections are calculated for pp collisions in the center-of-mass (CM) frame with energy $\sqrt{s} = 14$ TeV, and CTEQ6M [14] parton distributions functions are used to fold in the cross section for the hard partonic production processes.

From Eq. (4.2) we see that the only model parameters the production cross section explicitly depend on are v_T and the mixing angle δ . The dependence on all other model parameters are implicit through the dependence on the $P_1^{\pm\pm}$ mass, M_{P_1} , as given in Eq. (2.8). The choice we made in our calculations is thus to set

$$M = v_T, \quad \kappa_\Psi = -\kappa_2, \quad m = 2v = 492.442 \text{ GeV}, \quad \lambda = -\lambda'_T = \rho/2 = 1, \tag{4.3}$$

and vary M_{P_1} by varying κ_2 . Note that with this choice, s_δ is independent of κ_2 , and thus M_{P_1} . For the SM parameters, we take $v = 246.221$ GeV, $e = 0.3133$ and $s_W = 0.4723$.

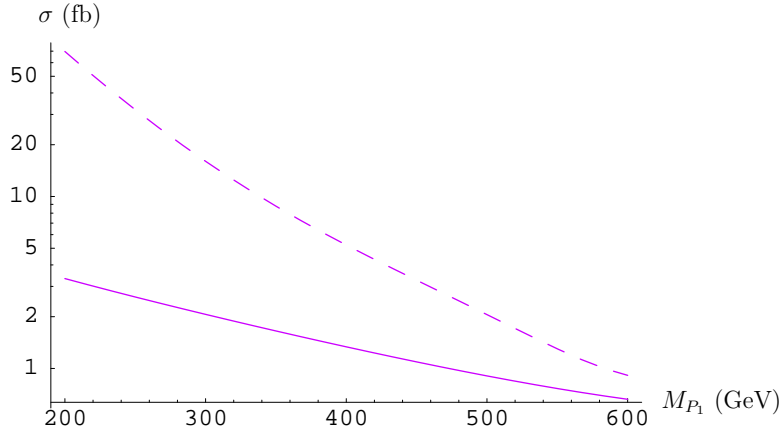


Figure 11: Production cross sections for $P_1^{\pm\pm}$ with $v_T = 4$ GeV and $s_\delta = 0.12$. The solid line traces the results from the W fusion processes, the dashed line the Drell-Yan annihilation processes.

We plot in Fig. 11 the production cross section for $P_1^{\pm\pm}$ from WW fusion and Drell-Yan pair annihilation as a function of M_{P_1} . Note that QCD corrections are expected to increase the DY production cross section by a factor of about 1.25 at next-to-leading order [15]. The CalcHEP results are checked with that calculated from PYTHIA [16], and are found to be consistent.

¶For couplings with P_2 , $c_\delta \rightarrow -s_\delta$, $s_\delta \rightarrow c_\delta$.

Except for the mixing angle factors c_δ and s_δ , the coupling of $P_1^{\pm\pm}$ to the weak gauge bosons are the same as that of $\Delta_L^{\pm\pm}$ to the W_L , Z_1 bosons in the left-right symmetric model [17], while the couplings to photon is the same in both models. Thus, the results for the cross section should agree once the scaling factors are taken into account. Comparing the results of our model to that of Refs. [18, 19], we find good agreements.

We see from Fig. 11 that DY pair production is dominant compared to the single production channel via WW fusion for the whole range of $P_1^{\pm\pm}$ masses in our model. This is a robust feature in the production of the doubly charged Higgs at hadron colliders in many models. This is because the virtual photon exchange is the same for all models and only the Z exchange term is model dependent, which is subdominant. The relative magnitude of production via WW fusion compared to the DY pair production can thus be used to distinguish between the different models containing the doubly charged Higgs.

4.2 The decay of $P_1^{\pm\pm}$

At the leading order, there are six decay channels possible for $P_1^{\pm\pm}$:

$$\begin{aligned}
(1) \quad & P_1^{\pm\pm} \rightarrow l_{aR}^\pm l_{bR}^\pm \quad (a, b = e, \mu, \tau), \\
(2) \quad & P_1^{\pm\pm} \rightarrow W^\pm W^\pm, \\
(3) \quad & P_1^{\pm\pm} \rightarrow P^\pm W^\pm, \\
(4) \quad & P_1^{\pm\pm} \rightarrow P^\pm P^\pm, \\
(5) \quad & P_1^{\pm\pm} \rightarrow W^\pm W^\pm X^0, \quad X^0 = T_a^0, h^0, P^0 \\
(6) \quad & P_1^{\pm\pm} \rightarrow P^\pm P^\pm X^0.
\end{aligned} \tag{4.4}$$

Kinematically, mode (4) and (6) are not allowed in our model, while the availability of the rest depends on the value of the scalar boson masses. The coupling for mode (2) has been given in Eq. (4.2), for mode (1), (3) and (5) the couplings are given by

$$\begin{aligned}
& P_1^{\pm\pm} l_{aR}^\mp l_{bR}^\mp : Y_{ab} s_\delta P_1^{--} \overline{l_{aR}^c} l_{bR} + h.c. \\
& P_1^{\pm\pm} W_\mu^\mp P^\mp : ig c_\delta W_\mu^- [\partial_\nu P_1^{++} P^- - P_1^{++} \partial_\nu P^-] + h.c. \\
& P_1^{\pm\pm} W_\mu^\mp W_\nu^\mp X^0 : \frac{g^2}{\sqrt{2}} c_X P_1^{\pm\pm} W_\mu^\mp W_\nu^\mp X^0 + h.c.
\end{aligned} \tag{4.5}$$

where $c_X = i, \cos \vartheta, \sin \vartheta$ for $X^0 = T_a^0, h^0, P^0$ respectively.

The leptonic decays are kinematically the most favorable mode of decay for the doubly charge Higgs, $P_1^{\pm\pm}$, and this is a universal feature in any model that contains them. The leptonic decay width has a very simple form given by

$$\Gamma(l_{aR}^\pm l_{bR}^\pm) = (1 + \delta_{ab}) \frac{|Y_{ab}|^2}{16\pi} s_\delta^2 M_{P_1} \quad (\text{no sum}). \tag{4.6}$$

Note that in our model, the final state charged leptons are right-handed. Hence in principle, helicity measurements can be used to distinguish between our model and those whose doubly charged Higgs coupling only to left-handed leptons (see e.g. [20, 21, 22, 23, 24]).

From the discussion above, it is not unreasonable to take $Y_{ab} \sim 0.1$ (except for $Y_{\tau\tau}$, which is constrained to be ten times smaller). Thus, provided the mixing angle between

the doubly charged Higgs bosons, δ , is not too small, one can expect spectacular signals from like-sign dileptons such as $e\mu$, $e\tau$ and $\mu\tau$, that are directly produced from $P_1^{\pm\pm}$.

The $W^\pm W^\pm$ channel opens up once $M_{P_1} > 2M_W$. Its decay width is

$$\Gamma(W^\pm W^\pm) = \frac{g^4 v_T^2 c_\delta^2}{16\pi M_{P_1}} \sqrt{1 - \frac{4M_W^2}{M_{P_1}^2}} \left(3 - \frac{M_{P_1}^2}{M_W^2} + \frac{M_{P_1}^4}{4M_W^4} \right), \quad (4.7)$$

which is proportional to v_T^2 . Given that v_T is small, and M_{P_1} is of order the electroweak scale, whether the leptonic or $W^\pm W^\pm$ mode dominates depends on the value of the mixing angle δ .

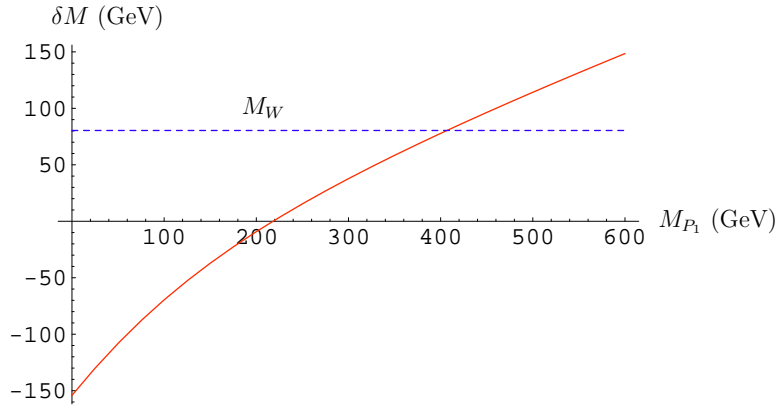


Figure 12: The mass difference $\delta M = M_{P_1} - M_P$ as a function of M_{P_1} for $v_T = 4$ GeV. The short dashed line marks where $\delta M = M_W$, which opens up the decay channel.

The $W^\pm P^\pm$ mode opens up once the mass difference, $\delta M = M_{P_1} - M_P$, where M_P is the mass of the singly charged Higgs boson, is greater than $2M_W$. From Eq. (2.7), we see that if M_P is to be of interest at the LHC, ω needs to be order unity (the validity of perturbation theory constrains $|\kappa_2|$ to be less than 4π). This implies that $M \sim v_T$, and in Fig. 12 we plot δM as a function of M_{P_1} for $M = v_T = 4$ GeV. We vary M_{P_1} the same way as detailed in Sec. 4.1, with the same choice of parameters, Eq. (4.3). For this choice, the decay channel opens up once $M_{P_1} > 407$ GeV.

The decay width for the $W^\pm P^\pm$ mode is given by

$$\Gamma(W^\pm P^\pm) = \frac{g^2 c_\delta^2 M_{P_1}^3}{16\pi M_W^2} \lambda^{\frac{3}{2}} \left(1, \frac{M_W^2}{M_{P_1}^2}, \frac{M_P^2}{M_{P_1}^2} \right), \quad (4.8)$$

where $\lambda(x, y, z) = x^2 + y^2 + z^2 - 2xy - 2xz - 2yz$. With a dependence of g^2 and no suppression coming from factors of v_T , the $W^\pm P^\pm$ mode is expected to dominate over the $W^\pm W^\pm$ mode once it becomes available. Note that the singly charged Higgs decays primarily into $W\gamma$ rather than fermion pairs, which is the dominant decay mode for the usual charged Higgs originating from SM doublets.

In general, the three-body decay mode $W^\pm W^\pm X^0$, $X^0 = T_a^0, h^0, P^0$, is expected to be relatively suppressed by the three-body phase space when compared to the two-body

modes. However, since the couplings do not depend on v_T , if $s_\delta \ll 1$, it may become important compared to the lepton and $W^\pm W^\pm$ modes.

The masses of the neutral pseudoscalar and scalar bosons, m_{X^0} , are given by Eqs. (2.14) and (2.15). Here too, $\omega \sim \mathcal{O}(1)$ is required to keep the neutral bosons at electroweak scale. Note that once ω is fixed, M_{X^0} and M_{P_1} are governed by independent sets of parameters. Below, we will choose $X^0 = T_a^0$ as the representative three-body mode, which has the least and simplest model dependence compared to the neutral scalar cases. The difference in the decay widths would come in only as ratios of masses, and from the neutral mixing angle factors, c_ϑ and s_ϑ .

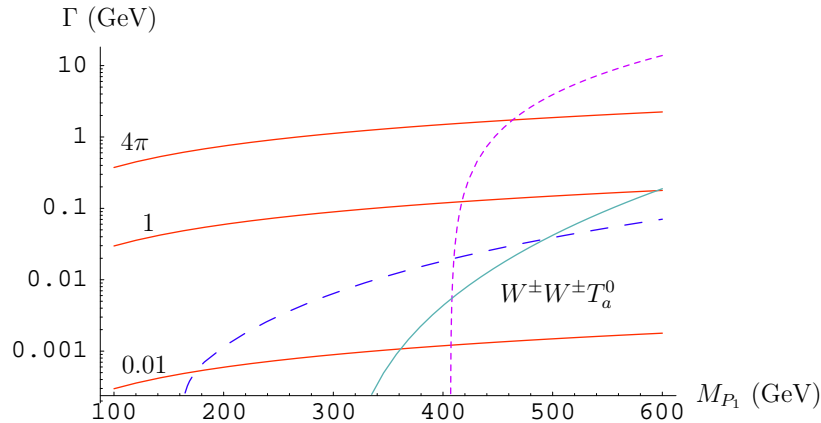


Figure 13: Decay widths of $P_1^{\pm\pm}$ as a function of M_{P_1} , with $v_T = 4$ GeV and the mixing angle fixed at $\sin \delta = 0.12$. The leptonic mode is represented by the solid lines at different values of $|Y_{ab}|^2$, the $W^\pm W^\pm$ mode the long dashed line, and the $W^\pm P^\pm$ mode the short dashed line. The three-body $W^\pm W^\pm T_a^0$ mode is labelled on the plot.

For the choice $M = v_T = 4$ GeV, $M_{T_a^0} = 146.5$ GeV, and the $W^\pm W^\pm T_a^0$ mode opens up once $M_{P_1} > 307.31$ GeV. Since there is no known closed form for the phase space of general three-body decays, we calculate the three-body decay widths numerically using CalcHEP as a function of M_{P_1} . We display the result and compared with all the allowed two-body modes listed in Eq. (4.4) in Fig. 13. We work in the small mixing scenario where $s_\delta = 0.12$, since for $s_\delta \sim 1$, the results are qualitatively that of the left-right symmetric models [17].

There are several noteworthy features. First, despite the phase space advantage, the suppression of the lepton mode by the s_δ^2 factor is such that the $W^\pm W^\pm$ mode is never negligible for $|Y_{ab}|^2 \sim 1$, and dominating for $|Y_{ab}|^2 \ll 1$ even for small values of M_{P_1} . Next as discussed above, the $W^\pm P^\pm$ mode dominates over both the lepton and $W^\pm W^\pm$ modes, and does so almost at once after it becomes kinematically available. Moreover, even if one were to push $|Y_{ab}|^2$ to the perturbative limit of 4π , the $W^\pm P^\pm$ mode would still become dominant soon above its threshold. Lastly, and perhaps most interestingly, the three-body $W^\pm W^\pm T_a^0$ mode dominates over the lepton mode when $|Y_{ab}|^2 \ll 1$ (suppression by s_δ), and is significant relative to the $W^\pm W^\pm$ mode and even overtakes it at large values of M_{P_1} (suppression by v_T).

These are features that are not shared by other doubly charged Higgs models, and will serve to distinguish our model from them at the LHC.

5. Conclusion

We have given a detail study of the phenomenology of a model where Majorana neutrino mass is induced radiatively at two-loop. This is made possible by extending the Higgs sector of the SM, and the new structure involves a triplet and a doubly charged singlet field. Lepton number is violated only in the scalar sector by a hard and a soft term. When these two terms are set to zero, the model conserves lepton number, and is technically natural.

Since the active neutrinos masses are two-loop effects due to new physics at the TeV scale, the model is testable at the LHC. In our study, we have focused on the production and decays of the doubly charged Higgs bosons. We find it is possible in the enlarged Higgs sector parameter space to have always at least one doubly charged Higgs with mass $\lesssim 600$ GeV. Furthermore, in much of the parameter space, two doubly charge Higgs can be expected to have masses within reach of the LHC. We find that Drell-Yan mechanism is the dominant production mechanism, with single production from WW fusion coming into play only for masses greater than 600 GeV. This is common to most doubly charged Higgs models. We find cross sections ranging from $\mathcal{O}(1 - 70)$ fb without including QCD effects, which typically cause an enhancement by a factor of 1.25.

The decays of the doubly charged Higgs are potentially the best way of differentiating between the different doubly charged Higgs models. We find that with reasonable values of the Yukawa couplings, the leptonic decays are not always dominant despite being kinematically favorable. Nevertheless, decay modes producing directly same sign dilepton pairs such as $e\tau$, $\mu\tau$, and $e\mu$, are distinctive and unmistakable. Moreover, since the doubly charged Higgs only couples to RH leptons in our model, their decays into a pair of tauons offer opportunities for helicity measurements. Another interesting feature of the doubly charged Higgs decays is that three-body modes $W^\pm W^\pm X^0$ involving the neutral scalar and pseudoscalar bosons can become as important as the two-body modes, particularly when the mixing between the doubly charged Higgs is small.

The model we studied here can only accommodate the normal hierarchy for the active neutrino mass matrix. It predicts that the first element to be very small. Moreover, $0\nu\beta\beta$ decays of nuclei can still occur via the exchange of doubly charged Higgs. This give rise to the interesting situation whereby if such decays are seen, the doubly charged Higgs will also be seen at the LHC, and vice versa. If the neutrino mass hierarchy turns out to be other than the normal hierarchy, neutrino masses are not generated by the model we studied.

Acknowledgments

We thank Dr. D. Axen for kindly sharing with us his knowledge and insights on PYTHIA, and Dr. G. Azuelos for useful discussions. This work is supported in part by the National

Science Council of R.O.C. under Contract No. NSC-95-2112-M-007-059-MY3, and by the Natural Science and Engineering Council of Canada.

References

- [1] K. R. Dienes, E. Dudas and T. Gherghetta, *Light neutrinos without heavy mass scales: A higher-dimensional seesaw mechanism*, *Nucl. Phys.* **B 557** (1999) 25 [[hep-ph/9811428](#)]; S. J. Huber and Q. Shafi, *Seesaw mechanism in warped geometry*, *Phys. Lett.* **B 583** (2004) 293.
- [2] A. Zee, *A Theory Of Lepton Number Violation, Neutrino Majorana Mass, And Oscillation*, *Phys. Lett.* **B 93** (1980) 389 [Erratum-ibid. **B 95** (1980) 461]; *Charged Scalar Field And Quantum Number Violations*, *Phys. Lett.* **B 161** (1985) 141.
- [3] G. L. Fogli, E. Lisi, A. Marrone and A. Palazzo, *Global analysis of three-flavor neutrino masses and mixings*, *Prog. Part. Nucl. Phys.* **57** (2006) 742 [[hep-ph/0506083](#)].
- [4] A. Zee, *Quantum Numbers Of Majorana Neutrino Masses*, *Nucl. Phys.* **B 264** (1986) 99; K.S. Babu, *Model of 'Calculable' Majorana Neutrino Masses*, *Phys. Lett.* **B 203** (1988) 132.
- [5] C. S. Chen, C. Q. Geng and J. N. Ng, *Unconventional neutrino mass generation, neutrinoless double beta decays, and collider phenomenology*, *Phys. Rev.* **D 75** (2007) 053004 [[hep-ph/0610118](#)].
- [6] W. M. Yao *et al.* [Particle Data Group], *Review of particle physics*, *J. Phys.* **G 33** (2006) 1.
- [7] O. Stelzer-Chilton [for the CDF Collaboration], *First Run II Measurement of the W Boson Mass with CDF*, [hep-ex/0706.0284](#).
- [8] M. C. Gonzalez-Garcia and Y. Nir, *Implications Of A Precise Measurement Of The Z Width On The Spontaneous Breaking Of Global Symmetries*, *Phys. Lett.* **B 232** (1989) 383.
- [9] J. van der Bij and M. J. G. Veltman, *Two Loop Large Higgs Mass Correction To The Rho Parameter*, *Nucl. Phys.* **B 231** (1984) 205; K. L. McDonald and B. H. J. McKellar, *Evaluating the two loop diagram responsible for neutrino mass in Babu's model*, [hep-ph/0309270](#).
- [10] K. S. Babu and C. Macesanu, *Two-loop neutrino mass generation and its experimental consequences*, *Phys. Rev.* **D 67** (2003) 073010 [[hep-ph/0212058](#)].
- [11] B. Pontecorvo, *Neutrino experiments and the question of leptonic-charge conservation*, *Sov. Phys. JETP* **26** (1968) 984; Z. Maki, M. Nakagawa, and S. Sakata, *Remarks on the unified model of elementary particles*, *Prog. Theor. Phys.* **28** (1962) 870.
- [12] M. Raidal and A. Santamaria, *μ -e conversion in nuclei versus $\mu \rightarrow e\gamma$: An effective field theory point of view*, *Phys. Lett.* **B 421** (1998) 250
- [13] A. Pukhov *et al.*, *CompHEP: A package for evaluation of Feynman diagrams and integration over multi-particle phase space. User's manual for version 33*, [hep-ph/9908288](#); A. Pukhov, *CalcHEP 3.2: MSSM, structure functions, event generation, batchs, and generation of matrix elements for other packages*, [hep-ph/0412191](#).
- [14] J. Pumplin, D. R. Stump, J. Huston, H. L. Lai, P. Nadolsky and W. K. Tung, *New generation of parton distributions with uncertainties from global QCD analysis*, *J. High Energy Phys.* **0207** (2002) 012 [[hep-ph/0201195](#)].

- [15] M. Mühleitner and M. Spira, *Note on doubly charged Higgs boson pair production at hadron colliders*, *Phys. Rev. D* **68** (2003) 117701
- [16] T. Sjostrand, S. Mrenna and P. Skands, *PYTHIA 6.4 physics and manual*, *J. High Energy Phys.* **0605** (2006) 026 [[hep-ph/0603175](#)].
- [17] J. F. Gunion, J. Grifols, A. Mendez, B. Kayser and F. I. Olness, *Higgs Bosons In Left-Right Symmetric Models*, *Phys. Rev. D* **40** (1989) 1546.
- [18] K. Huitu, J. Maalampi, A. Pietila and M. Raidal, *Doubly charged Higgs at LHC*, *Nucl. Phys. B* **487** (1997) 27 [[hep-ph/9606311](#)].
- [19] G. Azuelos, K. Benslama and J. Ferland, *Prospects for the search for a doubly-charged Higgs in the left-right symmetric model with ATLAS*, *J. Phys. G* **32** (2006) 73 [[hep-ph/0503096](#)].
- [20] J.A. Coarasa, A. Méndez, and J. Solà, *Higgs triplet effects in purely leptonic processes*, *Phys. Lett. B* **374** (1996) 131.
- [21] A. G. Akeroyd and M. Aoki, *Single and pair production of doubly charged Higgs bosons at hadron colliders*, *Phys. Rev. D* **72** (2005) 035011 [[hep-ph/0506176](#)].
- [22] A. G. Akeroyd, M. Aoki and Y. Okada, *Lepton Flavour Violating tau Decays in the Left-Right Symmetric Model*, [hep-ph/0610344](#).
- [23] A. Hektor, M. Kadastik, M. Muntel, M. Raidal and L. Rebane, *Testing neutrino masses in little Higgs models via discovery of doubly charged Higgs at LHC*, [hep-ph/0705.1495](#).
- [24] T. Han, B. Mukhopadhyaya, Z. Si and K. Wang, *Pair Production of Doubly-Charged Scalars: Neutrino Mass Constraints and Signals at the LHC*, [hep-ph/0706.0441](#).